Sensors and Actuators A 176 (2012) 64–71

Contents lists available at SciVerse ScienceDirect

Sensors and Actuators A: Physical

journal homepage: www.elsevier.com/locate/sna

Functionalized individual ZnO microwire for natural gas detection

G.Y. Chai[a], O. Lupan[a,b,*], E.V. Rusu[c], G.I. Stratan[c], V.V. Ursaki[d,e], V. Şontea[b], H. Khallaf[a], L. Chow[a,f,g]

[a] Department of Physics, University of Central Florida, PO Box 162385, Orlando, FL 32816-2385, USA
[b] Department of Microelectronics and Semiconductor Devices, Technical University of Moldova, 168 Stefan cel Mare Blvd., MD-2004 Chisinau, Republic of Moldova
[c] Laboratory of Nanotechnology, Institute of Electronic Engineering and Nanotechnology, Academy of Sciences of Moldova, MD-2028 Chisinau, Republic of Moldova
[d] Institute of Applied Physics of the Academy of Sciences of Moldova, MD-2028 Chisinau, Republic of Moldova
[e] National Center for Materials Study and Testing, Technical University of Moldova, Chisinau 2004, Republic of Moldova
[f] Graduate Institute of Electro-Optical Engineering and Green Technology Research Center, Chang Gung University, Taiwan
[g] Advanced Materials Processing and Analysis Center, and Department of Mechanical, Materials, and Aerospace Engineering, University of Central Florida, PO Box 162385, Orlando, FL 32816-2455, USA

ARTICLE INFO

Article history:
Received 16 September 2011
Received in revised form 6 January 2012
Accepted 8 January 2012
Available online 16 January 2012

PACS:
81.05.Dz II–VI semiconductors

Keywords:
ZnO microwire
Sensor
Natural gas
Methane
Focused ion beam

ABSTRACT

A single ZnO microwire detector for the monitoring of natural gas species is described. Single-crystal ZnO microwires were synthesized using a carbothermal reduction vapor phase transport method. It was characterized by XRD, EDX, SEM, Raman and photoluminescence techniques. The sensor structure was fabricated by in situ lift-out method using focused ion beam (FIB) system. The prototype is then functionalized with palladium and used as sensing element. The main advantage of the FIB procedure is a quick verification/testing of concept and is compatible with micro/nanoelectronic devices. A response of 5% was obtained for a single ZnO microwire sensor at 2000 ppm natural gas in the air at room temperature. At 400 °C the response increases to 40%. Selectivity to different gasses was investigated and higher response was detected for natural gas.

1. Introduction

Natural gas (NG) is an important feedstock for potential residential fuel cell systems because the infrastructure to supply natural gas is already established and the technology for producing hydrogen from natural gas [1] is available. The majority of current natural gas sensors are based on the catalytic mechanism of operation. The obvious drawback of these types of sensors is that they can be easily poisoned by halogens and halogen derivatives. The oxide semiconductor (SnO_2, ZnO, etc.)-based natural gas sensors showed excellent response and recover characteristics and can potentially overcome obstacles, such as sensitivity and selectivity [2–6]. Among various materials, ZnO is one of the most promising multifunctional materials for NG sensors due to its advantageous features, such as high sensitivity under ambient conditions, low-cost and simplicity in synthesis. Few data on ZnO as sensing material for natural gas were reported previously. Wang et al. [7] reported on thermal desorption spectroscopy TDS and adsorption probability measurements of iso-butane on the Zn-terminated surface of ZnO. Mazingue et al. [8] reported on optogeometric properties of ZnO sensitive thin films involved in butane gas sensing and on the butane sensing using ZnO-nanostructured coatings prepared by pulsed laser deposition [9]. Lupan et al. [10] investigated gas response of an individual ZnO tetrapod-based sensor to CH_4 gas at 100 ppm concentration. Lee et al. [11] studied the ZnO nanorod-coated quartz crystals as self-cleaning thiol sensors for natural gas fuel cells and their results highlight the potential of ZnO nanorod-grown quartz crystal microbalance as self-cleaning sensors capable of long-term operation under harsh conditions. Kim et al. [12] demonstrated possibility to develop on oxide films propane/butane gas sensor with low power consumption (as low as 100 mW) for the application to portable gas detection devices. However, no reports on the natural gas using individual Pd-functionalized ZnO microwire were found in the literature.

ZnO nanorods/nanowires have been grown by a variety of methods such as pulsed laser deposition [13], vapor phase transport process [14], chemical vapor deposition method [15].

* Corresponding author. Tel.: +1 407 823 2333; fax: +1 407 823 5112.
E-mail addresses: guangyuchai@yahoo.com (G.Y. Chai), lupan@physics.ucf.edu, lupanoleg@yahoo.com (O. Lupan), rusue@nano.asm.md (E.V. Rusu), ursaki@yahoo.com (V.V. Ursaki), sontea@mail.utm.md (V. Şontea), hani@physics.ucf.edu (H. Khallaf), Lee.Chow@ucf.edu (L. Chow).

0924-4247/$ – see front matter © 2012 Elsevier B.V. All rights reserved.
doi:10.1016/j.sna.2012.01.012

More recently, the solution chemical route has been reported as a low-cost, low-temperature method of ZnO synthesis [16,17]. However, the nano-size makes the ZnO sensing devices difficult to survive under extreme environments. In order to develop reliable ZnO-based gas sensing devices, the high-quality zinc oxide microwires [18,19] are employed to optimize the NG sensing performance.

Here, we demonstrate a single ZnO microwire can be used to fabricate a NG detector. This study shows a simple and cost-effective method to fabricate low-dimensional ZnO device, possibly leading to a next generation of oxide semiconductor gas sensors for a wide range of applications.

2. Experimental

The carbothermal reduction vapor phase transport growth of ZnO microwire structures was carried out in a horizontal furnace with an argon/oxygen flow as described elsewhere [18]. The argon and oxygen flow rates were set as 60 sccm and 200 sccm, respectively. A mixture of ZnO (99.99%) and graphite (99.999%) powder in ratio of 1:1 was used as a source material placed in an inner quartz tube of the end opposite to the entrance of the gas flow. A temperature profile with the maximum of 1030 °C at the source material and 1000 °C at the substrate was set in the furnace with the temperature gradient in the direction opposite to the gas flow. A Si or Al_2O_3 substrate was placed at the distance of 1 cm up-stream from the source material (i.e. in the direction opposite to the gas flow). The growth process was performed during a 1–2 h period of the time.

The crystalline quality and orientations of as-prepared ZnO structures were analyzed by X-ray diffraction (XRD) using a Rigaku 'D/B max' X-ray diffractometer (Cu K_α radiation source with $\lambda = 1.54178$ Å). The operating conditions were 30 mA and 40 kV at a scanning rate of 0.04°/s. The morphology of the products was analyzed by scanning electron microscopy (SEM). The ZnO wires were characterized by energy dispersion X-ray spectroscopy (EDX). The morphology is considered to play a vital role in device applications. The continuous wave photoluminescence (PL) was excited by the 351.1 nm line of a Spectra Physics Ar^+ laser and analyzed with a double spectrometer ensuring the spectral resolution better than 0.5 meV. The samples were mounted on the cold station of a LTS-22-C-330 optical cryogenic system. The Raman scattering (RS) measurements were carried out at room temperature with a MonoVista CRS Confocal Laser Raman System in the backscattering geometry under the excitation by a 532 nm DPSS laser. An in situ lift-out technique was used for the device fabrication in a focused ion beam (FIB) instrument. Before being integrated in sensor structure microwires were dipped in a 20 mM $PdCl_2$ in ethanol and afterwards thermal treated at 400 °C. The gas response was measured using a two-terminal ZnO microwire device [19,20]. Its characteristics were measured using a semiconductor parameter analyzer with input impedance of 2.00×10^8 Ω. The fabricated device structure was put in an environmental chamber to detect different gasses (H_2, O_2, C_2H_5OH, CO, CO_2 and natural gas (NG)). The humidity of the gas mixture was about 60%RH. The gas flow was controlled by MKS mass flow controller and test system as reported before [10,21,22].

3. Results and discussion

Fig. 1 shows an SEM micrograph of microwires grown at an oxygen flow rate of 60 sccm and at a temperature ramp-up rate of 30 °C/min. The average length and diameter of these ZnO microwires are 50–200 μm and 1–3 μm, respectively. It was also found that the cross-section of the ZnO microwires was well

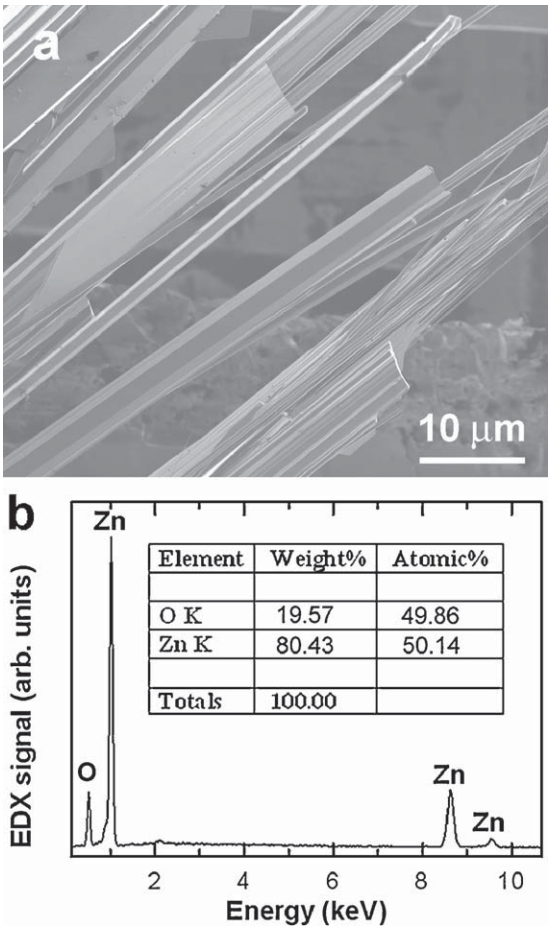

Fig. 1. (a) SEM image of the ZnO microwires synthesized by carbothermal reduction vapor phase transport; and (b) the EDX analysis of ZnO microwires.

-defined hexagons. The EDX analysis of the produced structures demonstrates a stoichiometric ZnO composition in the limits of the sensitivity of the EDX system. We found that the Zn:O ratios in our nanostructures to be 50.1:49.9 atomic ratio in all samples (Fig. 1b).

Fig. 2 presents the XRD patterns of the ZnO microwires that are shown in Fig. 1a. It can be seen that all diffraction peaks are from crystalline ZnO with the hexagonal wurtzite structure. The narrow peak width at (0 0 2) indicates that *c*-axis of the microwires are

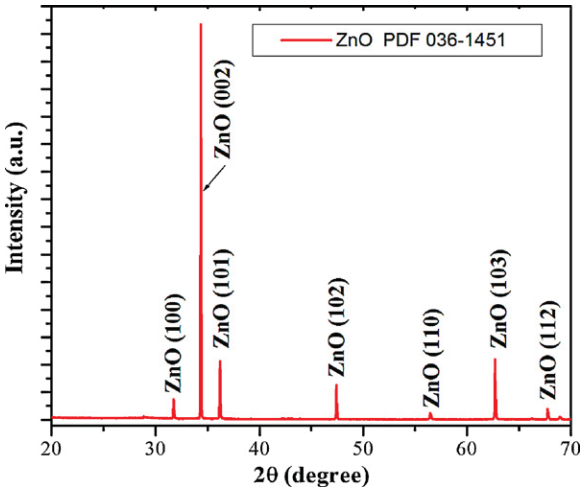

Fig. 2. Typical XRD pattern of the ZnO microwires.

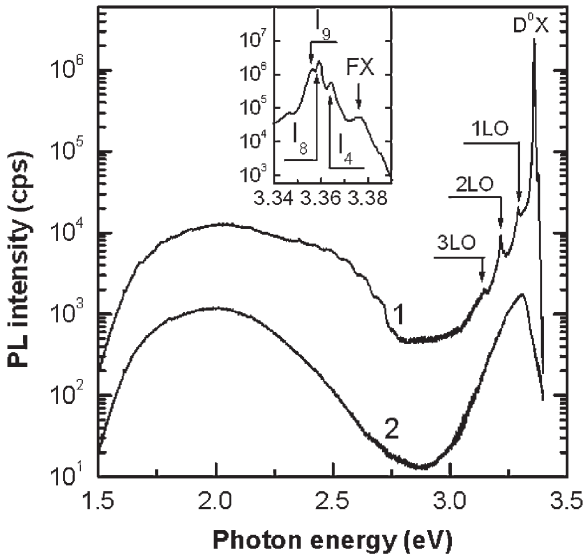

Fig. 3. Photoluminescence spectrum measured at: (1) 10 K; and (2) 300 K. The inset is the detailed presentation of the excitonic luminescence at 10 K.

well aligned along the growth direction. The lattice constants a and c were determined as $a = 0.325$ nm, $c = 0.520$ nm by using the following equation [16]:

$$\frac{1}{d^2_{(h\ k\ l)}} = \frac{4}{3}\left(\frac{h^2 + hk + k^2}{a^2}\right) + \frac{l^2}{c^2}. \quad (1)$$

The lattice parameter $d(0\,0\,2)$ value of the produced ZnO is 2.60 Å which is the same as that of the un-stressed ZnO bulk. All observed Bragg reflections are consistent with the Wurtzite $P6_3mc$ space group.

The PL of the material produced consists of a series of emission lines in the near-band-edge spectral region, and two PL bands with central positions at 2.5 eV and 2.0 eV in the visible spectral range (Fig. 3). Note that the intensity of the near-band-edge emission (NBE) at low temperature (10 K) is two orders of magnitude higher than the intensity of the visible luminescence. The near-band-edge luminescence is dominated by the emission related to the recombination of donor bound excitons (D^0X) [23,24] with a series of LO phonon replica (Fig. 3). D^0X lines (see the inset in Fig. 3) are identified as previously reported I_4, I_8, and I_9 lines. The presence of a PL band related to the recombination of free excitons is indicative of a high optical quality of the material. With the increase of the temperature, the donor bound exciton luminescence sharply decreases due to the small binding energy of excitons. As a result, at high temperatures the near-band-edge PL is dominated by the recombination of free excitons which produces a PL band with the maximum at 3.3 eV.

The non-polarized micro-Raman spectrum measured in backscattering geometry from the cross-section of a bunch of the produced ZnO microwires in the direction parallel to the optical axis (i.e. in the z-direction) is presented in Fig. 4a. This spectrum demonstrates the good quality of the wurtzite crystal structure in the produced material. Wurtzite ZnO belongs to the C_{6v} space group ($P6_3mc$). According to group theory, the corresponding zone center optical phonons are $A_1 + 2B_1 + E_1 + 2E_2$ [25]. The $A_1 + E_1 + 2E_2$ modes are Raman active, while $2B_1$ are silent. The low-frequency E_2 mode is predominantly associated with the non-polar vibration of the heavier Zn sublattice, while the high frequency E_2 mode involves predominantly the lighter oxygen atoms. The A_1 and E_1 modes are split into LO and TO components. Except for the LO modes, and the low frequency E_2 mode which is outside the range

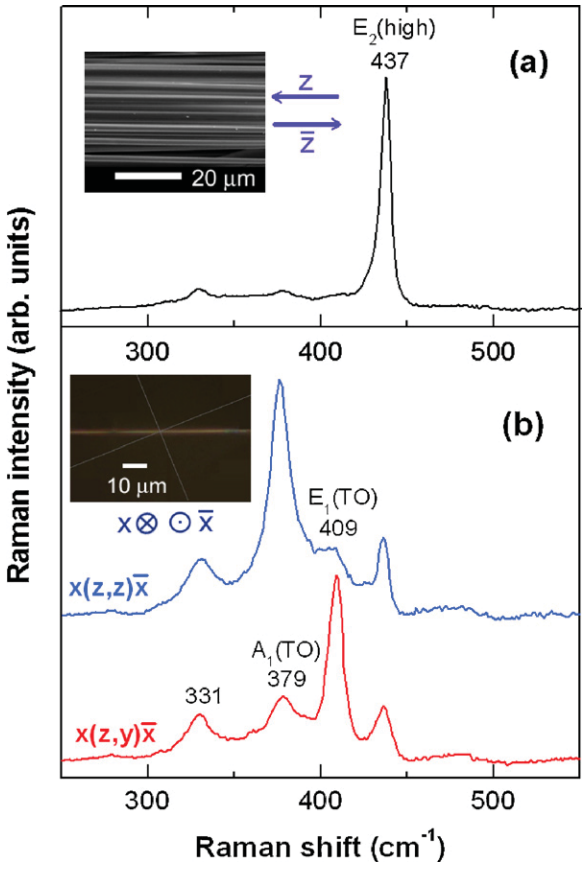

Fig. 4. (a) Room-temperature micro-Raman spectrum of a ZnO microwire bunch; and (b) a single ZnO microwire measured in backscattering geometry. A typical SEM image of the ZnO microwire bunch is shown as inset in (a), and a CCD image of the confocal Raman microscope of a single ZnO microwire is shown as inset in (b). The non-polarized spectrum in (a) is measured in the z-direction, while the polarized spectrum in (b) is measured in the x-direction.

of the presented Raman shifts, all Raman active phonon modes are clearly identified in the spectrum. The LO modes are not visible in the spectrum, likely due to the presence of a high free carrier concentration in the sample [14,26]. The peak at 331 cm^{-1} E_{2H}–E_{2L} is attributed to second order Raman processes involving acoustic phonons [27]. The intensity of the high-frequency E_2 mode is much higher as compared to the intensity of A_1(TO) and E_1(TO) modes, since the high-frequency E_2 mode is allowed in this geometry, while the A_1(TO) and E_1(TO) modes are forbidden. The presence of weak A_1(TO) and E_1(TO) modes in the spectrum of Fig. 4a is due to the deviation from a true backscattering geometry. The peak corresponding to E_2(high) mode has a linewidth of about 6 cm^{-1} which is comparable to values reported for high quality ZnO bulk crystals [28]. The position of the E_2 (high) peak corresponds to the phonon of a bulk ZnO crystal indicating a strain-free state of the nanowire. Therefore, the predominance of the E_2 mode demonstrates a highly oriented growth of ZnO microwires along the optical axis. This suggestion is confirmed also by the analysis of the polarized RS spectrum measured from a single ZnO microwire in backscattering geometry in the x-direction (i.e. perpendicularly to the microwire axis) as shown in Fig. 4b. One can see that in the (z,z) polarization for which the A_1(TO) is allowed and the E_1(TO) is forbidden, the intensity of the A_1(TO) phonon is by a factor of 5 higher as compared with the E_1(TO) phonon. An inverse ratio is observed for the (z,y) polarization for which the E_1(TO) is allowed and the A_1(TO) is forbidden. The presence of the E_2(high) mode in the spectrum of Fig. 4a is also due to the deviation from a true backscattering geometry.

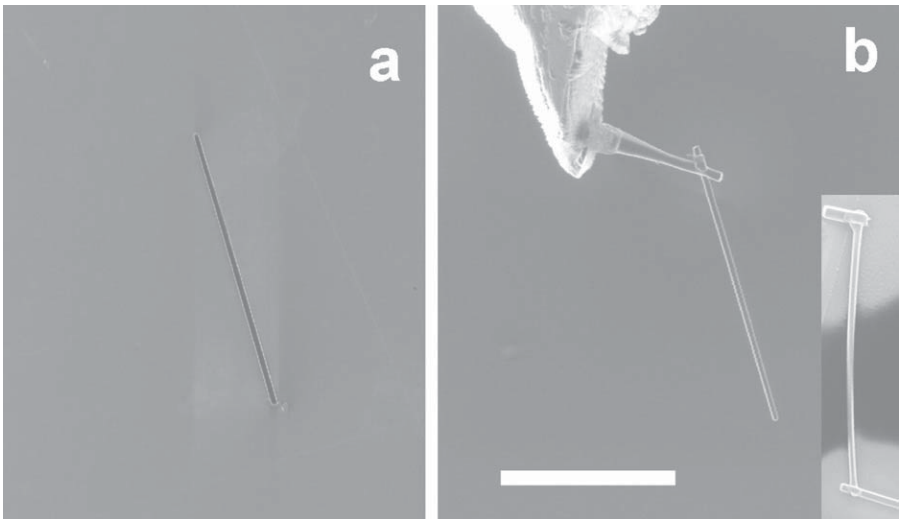

Fig. 5. In situ lift-out fabrication of the single ZnO microwire NG sensor. (a) Individual ZnO microwire transferred to Si/SiO_2 substrate; (b) FIB needle was attached ZnO microwire to be used as a sensor. Inset in (b) shows a mirowire connected to Au/Ti electrode. The scale bar is 20 μm.

The in situ lift-out technique has been used to fabricate the ZnO hydrogen sensors [29,30] and UV photodetector [19,20]. The process was done in an FIB chamber and more details can be found in [10,19,29,30]. To improve the sensing characteristics, the possibility of functionalization of microwire surface has been investigated. As mentioned above, ZnO microwires were dipped in a palladium chloride solution and thermal treated at 400 °C before in situ lift-out fabrication process for sensor structure. Afterwards, the zinc oxide microwire samples were first transferred onto the intermediate Si/SiO_2 substrate in order to reduce the sample density and avoid charging problems in the FIB system (Fig. 5a). Next, an electro-etched tungsten needle mounted on the micromanipulator was lowered and brought into the FIB focus to approach an intermediate ZnO microwire sample. The needle was moved until in contact with the microwire. Then the microwire was attached to the end of the FIB needle by ion beam assisted Pt deposition. The next step was to scan the Si/SiO_2 substrate for well-placed ZnO microwire. Once a desired microwire was identified the needle is used to pick up the ZnO microwire and the ZnO specimen was removed away from the substrate (Fig. 5b).

For the gas sensor structure preparation, a glass substrate was used and Au/Ti electrodes were sputter deposited as template with external electrodes/connections. The gap between the electrodes was about 20 μm. With the help of a micromanipulator, the ZnO microwire was placed across the substrate electrode gap. Then, the Pt deposition was applied to attach both ends of the ZnO microwire to the Au/Ti electrodes (Fig. 5b insert). In the final step, the microwire was cut from the anchor point (end of the intermediate ZnO microwire) and the needle was raised away from the substrate. The typical time to perform this in situ lift-out FIB fabrication is about 20–30 min.

The fabricated single ZnO microwire gas sensor was put in a test chamber to detect natural gas and other gasses, such as H_2, O_2, CO_2, CO and ethanol at room temperature. The gas response was defined as the ratio [29]:

$$S \approx \left|\frac{\Delta R}{R}\right|, \quad (2)$$

where $|\Delta R| = |R_{air} - R_{gas}|$ and R_{air} is the resistance of the sensor in dry air (~70 kΩ) and R_{gas} is resistance in the test gas.

We found that sensor structure has a gas response of less than 1.25% for H_2, O_2, CO_2, CO and ethanol under the same conditions. The maximum gas response (about 5%) was obtained for 2000 ppm of natural gas at room temperature. These data will be discussed next. The room-temperature natural gas response of the single ZnO microwire NG sensor is shown in Fig. 6.

According the results presented in Fig. 6 when the 2000 ppm natural is used, the response ($\Delta R/R$) increases about 5% within 30 s (from 10% to 90% of $\Delta R/R$). Afterwards, the NG gas is turned off and the detector resistance returns back to the initial value.

Fig. 7a shows the temperature dependence of NG response of the fabricated single ZnO microwire sensor structure. We can see that different operating temperatures of ZnO sensor lead to different responses to NG with a maximum at about 400 °C. This observation could be explained by the phenomena that at elevated operating temperature methane more easily decompose in species [31,32] and by catalytic reaction of the gas, which favor increase of response. According to results presented in Fig. 7a at temperatures >440 °C gas response starts to decrease. This phenomenon is due to the catalytic reaction of the gas. Each gas would require a certain optimum temperature to fully undergo the catalytic reaction. However, in our published work we have reported [30] on the observed hydrogenation effects for CVD ZnO nanowires lead to passivation of DL states and influence their properties. These effects must be taken into account when analyzing long-term stability of nanosensors

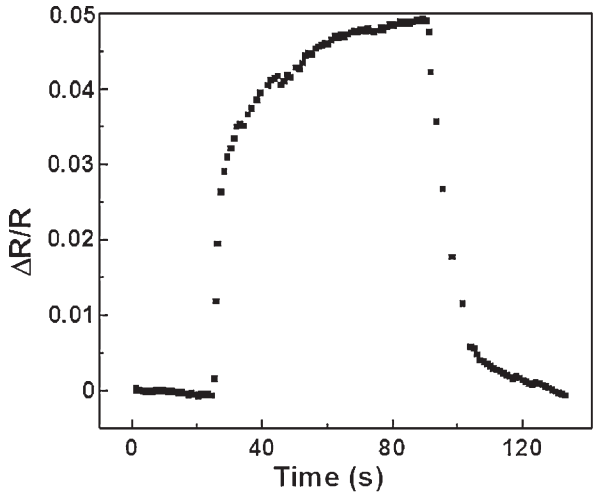

Fig. 6. Natural gas response measurement of the fabricated single ZnO microwire device at room temperature.

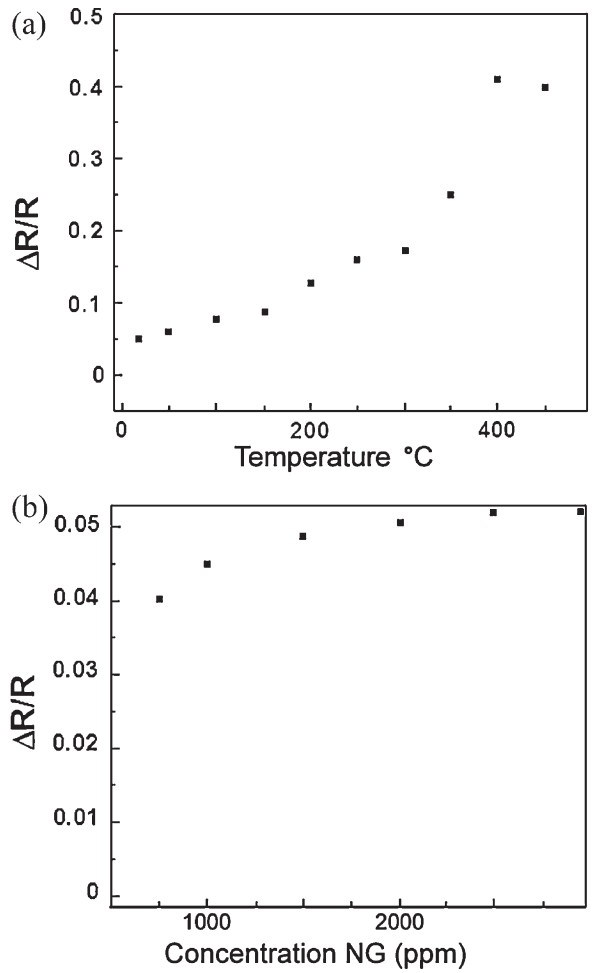

Fig. 7. (a) Temperature dependence of natural gas response measurement of a single ZnO microwire. (b) Dependence of gas response versus concentration of the natural gas measured from a single ZnO microwire at room temperature.

made on a single ZnO nanowire/microwire. Also, it is necessarily to mention that thermal annealing at temperatures higher than 400 °C in hydrogen atmosphere conduct to Zn reduction in ZnO [29,30]. That is why the main goal of our research was to develop a NG sensor working at room temperature. Fig. 7b shows the dependence of gas response versus concentration (750–3000 ppm) of the natural gas measured by a single ZnO microwire at room temperature. It can be seen that the value of $\Delta R/R$ increases from 4% to 5.2% with increasing NG concentration from 750 ppm to 3000 ppm at room temperature. For the methane sensors concentrations of interest are 1–100%LEL{Lower-Explosive-Limit} (which is 0.05–5% Volume corresponding to 500–50,000 ppm).

The possible mechanism for natural gas sensing could be described as follows. The oxygen adsorption on a zinc oxide surface could be as O_2^-, O^-, and O^{2-} ions due to a reaction followed by extracting electrons from the conduction band [33,34]. It is known that for individual ZnO microwires the oxygen adsorption and desorption dynamics depends sensitively on the concentration of surface oxygen vacancies [35,36]. It could have direct influence on the electron density of ZnO microwire and the adsorption process can be described as follows:

$$V_O + \frac{1}{2}O_{2(gas)} + 2e^- \leftrightarrow O^{2-}(ads). \quad (3)$$

The gas sensing mechanism can be explained by the charge transfer due to adsorption/desorption of an oxygen species on surface. Sensing mechanism is based on interaction between negatively charged oxygen adsorbed on the zinc oxide surface and the gas molecules.

The molecular oxygen is adsorbed on the ZnO surface and the electrons are consumed following the reactions:

$$O_2(gas) \leftrightarrow O_2(ads) + * \leftrightarrow O_2(ads) + e^- \leftrightarrow O_2{}^-(ads), \quad (4)$$

where * shows an available surface adsorption site. Other species of charged oxygen which exists on surface could be described in a simplified way:

$$O_2(gas) \leftrightarrow 2O(ads) + * \leftrightarrow 2O(ads) + 2e^- \leftrightarrow 2O^-(ads). \quad (5)$$

Thus, the extraction of electrons reduces the available free electrons and resistance increases.

It is of importance to consider the effect of H_2O in air too. The water vapors are adsorbed at the surface in molecular or hydroxyl forms and can react with the Zn sublattice and donate electrons as follows:

$$H_2O + O_O + 2Zn_{Zn} \leftrightarrow 2(OH{-}Zn) + V_O^{\bullet\bullet} + 2e^-, \quad (6)$$

where O_O is the oxygen in the lattice site, and $V_O^{\bullet\bullet}$ is the doubly charged vacancy at this site. According to this equation the resistivity decreases due to the formation of free electrons.

On the ZnO microwire surface, CH_4 is dissociated into CH_2^+ or CH_3^+ species and hydrogen. It is important to note that CH_4 is about 98% in natural gas, other 2% are C_2H_6, C_3H_8, C_4H_{10}, C_5H_{12}, CO_2, etc. This decomposition intensifies the adsorption of CH_4 radicals on the surface of ZnO and undergoes chain reactions. These reactions could be attributed to the Joule heat effect [37]:

$$CH_4 + O^{2-}{}_{ad} \rightarrow CH_2{}^+ + 2H^- + 3O^{2-} \rightarrow CO_2 + H_2O + 2H^- + 5e^- \quad (7)$$

$$CH_4 + O^{2-}{}_{ad} \rightarrow CH_3{}^+ + H^- + 7/2O^{2-} \rightarrow CO_2 + 3/2H_2O + H^- + 6e^- \quad (8)$$

$$CH_4 + 4O^{2-}{}_{ad} \rightarrow CO_2 + 2H_2O + 8e^- \quad (9)$$

$$C_3H_8 + 5O^{2-}{}_{ad} \rightarrow 3CO_2 + 4H_2O + 10e^- \quad (10)$$

Based on these reactions it is concluded that due to natural gas reaction with adsorbed oxygen 5, 6, 8 or 10 free electrons (e^-) are released. If compare with hydrogen reaction on the surface [33]

$$H_2 + O^{2-}{}_{ad} \rightarrow H_2O + 2e^- \quad (11)$$

only two free electrons ($2e^-$) are released back into conduction band. In this way the larger variation of the electrical resistance and the higher response value to NG in comparison to H_2 gas can be explained.

Hydrocarbon is dissociated on ZnO surface or on the surface of noble metal clusters before reacting with ionosorbed oxygen. We believe that palladium on the surface of zinc oxide microwire can improve the gas response and the rate of response due to catalytic activity for oxidation of natural gas (see inset in Fig. 8). Functionalization will increase the depletion region of surface, which will decrease rapidly when exposed to natural gas. This will explain the electron transport which can be seen in our NG response curve (Fig. 6). Several devices were fabricated using Pd–ZnO wires with radii between 400 nm and 1000 nm, which showed reproducible electrical responses in experiments repeated over a period of five months.

Fig. 8 shows the dependences of gas response for different gasses (H_2, O_2, CO_2, CO and ethanol under the same conditions) at two operating temperatures (400 °C and 22 °C) for a functionalized individual Pd–ZnO microwire and for a pure ZnO microwire (400 nm in diameter). For comparison the gas response of different diameters ZnO microwire gas sensors were also shown. Insert in Fig. 8 shows a

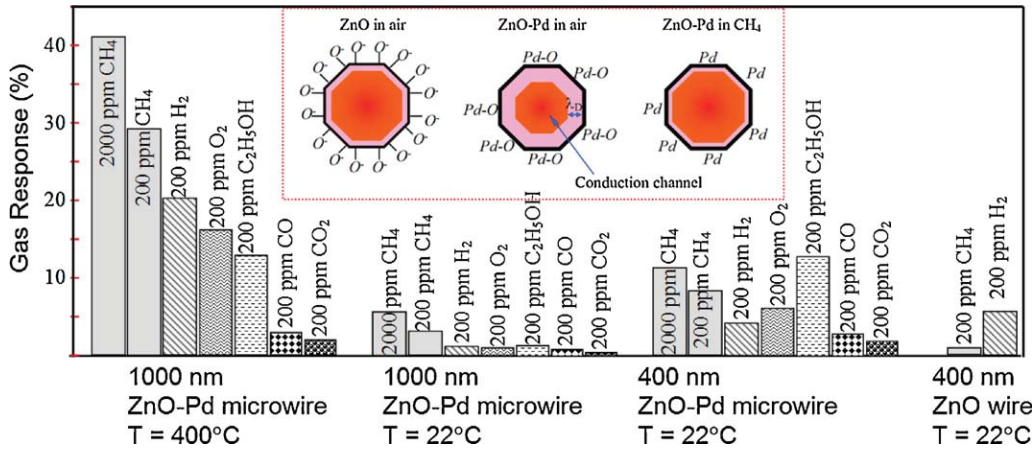

Fig. 8. Gas response of the single ZnO microwire gas sensor for different gasses, operating temperatures and diameters. Inset shows schematic cross-sectional view of pure ZnO microwire (left) and Pd-functionalized ZnO microwire (middle and right) with different length of the depleted region (λ_D).

cross-sectional view of pure ZnO microwire and Pd-functionalized ZnO microwire with different length of the depleted region (λ_D). It explains the proposed sensing mechanism of an individual ZnO microwire gas sensor exposed to air and to CH_4. More details on the sensing mechanism complementary to the proposed above can be found in our recent work [30]. The highest gas response (about 41% and about 5.2% at 400 °C and 22 °C, respectively) was obtained from a sensor based on a single Pd -functionalized ZnO microwire with a diameter of 1000 nm. For comparison, 400 nm wire shows a gas response to CH_4, less than 12% in case of Pd-functionalization of ZnO individual microwire and <0.34% for pure ZnO microwire, respectively. Our results demonstrate the importance of using thinner and functionalized microwires to design highly sensitive CH_4 sensors, which can operate without need of elevated temperatures. However, according to results presented in Fig. 8 with lowering the microwire diameter will decrease the NG selectivity of the ZnO microwire sensor. From Fig. 8, the 400 nm wire shows a higher sensitivity to ethanol than to CH_4 gas at room temperature. This means that even if sensitivity of a 400 nm wire is higher than of a 1000 nm wire, it will not distinguish CH_4 between several gas species. At the same time it is important to mention that our tests results at 400 °C demonstrates that samples with a 400 nm wire are not stable (resistance changes) after each run, which means that sensor performances decreases. This can be explained by hydrogenation effects for ZnO wires which influence their properties. Also, the sensing tests of samples at temperatures higher than 400 °C in hydrogen atmosphere result in Zn reduction in ZnO [29,30]. This phenomenon is more evident for micro/nanowires with diameters lower than 400 nm as was reported before by Lupan et al. [30]. Therefore we did not include results for 400 nm ZnO wires at 400 °C.

Fig. 8 (insert) describes the existence of the depletion layer of space charges at the microwires surface can explain the diameter-size dependent sensitivity behavior quantitatively. Insert in Fig. 8 shows cross-sectional view of pure ZnO microwire and Pd-functionalized ZnO microwire with different length of the depleted region (λ_D). It is clearly shown the suppression of the conduction channel by the Pd-functionalization of ZnO microwire. By introducing of such Pd–ZnO microwire in CH_4 the depletion layer will decrease affecting the conduction channel diameter as shown schematically in inset of Fig. 8. Another effect is that Pd facilitates the dissociation of CH_4 into ionized chemical species as discussed above.

The improvement of response time, selectivity and sensitivity to CH_4 by Pd functionalization of an individual ZnO microwire observed in Figs. 6–8, is most likely related to the acceleration of the adsorption, reactions and changes of the conduction channel

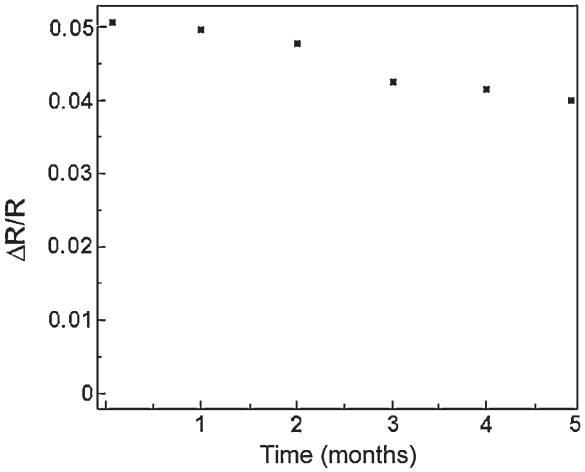

Fig. 9. Stability of an individual ZnO microwire sensor structure in time.

for different wires. We are working on further improvement of the gas response and selectivity by functionalization. Studies on the long term stability were performed. In Fig. 9 the sensing structure shows decreasing trend after 5 months of life at room temperature. It is important to mention that microwire was not protected from environment for this period. However, the results are promising for device applications. A comparison with previous work on an individual ZnO tetrapod sensor and its CH_4 gas detection performances [10] show a clear improvement of the sensitivity and selectivity after functionalization of a zinc oxide microwire.

The selectivity (e.g. cross response) is one of important gas-sensing issues for oxide microwire gas sensors [38]. The selectivity between NG, CO and H_2 is still one of the major problems for applications of such sensors due to same reducing character of gasses. Preliminary results have been presented in Fig. 8. At the same time we would like to mention that the response ($\Delta R/R$) decreases about 15% at room temperature with increase of relative humidity from 60%RH to 97%RH.

We consider that the properties of the sensing element (individual ZnO microwire) can be largely enhanced and the large-scale fabrication requirements can be satisfied.

4. Conclusions

In this work, a single ZnO microwire natural gas sensor structure for the monitoring of natural gas is demonstrated. The ZnO

microwire material was synthesized with carbothermal reduction vapor phase transport method. The SEM and XRD results show the high quality of the ZnO single crystal structure. FIB in situ lift-out technique is applied to fabricate the single microwire NG detector. It has been detected gas response of less than 1.25% for H_2, O_2, CO_2, CO and ethanol under the same conditions. The maximum gas response (about 5%) was obtained for natural gas at room temperature. The functionalized ZnO microwire sensor shows reliable NG response at room temperature. It was found the value of gas response increases from 4% to 5.2% with increasing NG concentration from 750 ppm to 3000 ppm at room temperature. Its temperature dependence was investigated and presented. Natural gas detection mechanism was proposed and discussed in details.

Acknowledgments

L. Chow acknowledges partial financial support from US Department of Agriculture award #58-3148-8-175. Financial support by the Supreme Council for Science and Technological Development of the Academy of Sciences of Moldova (Projects 036/R and 020RoF) is gratefully acknowledged.

References

[1] K. Blok, R.H. Williams, R.E. Katofsky, C.A. Hendriks, Hydrogen production from natural gas, sequestration of recovered CO_2 in depleted gas wells and enhanced natural gas recovery, Energy 22 (1997) 161–168.
[2] A. Chen, S. Bai, B. Shi, Z. Liu, D. Li, C.C. Liu, Methane gas-sensing and catalytic oxidation activity of SnO_2–In_2O_3 nanocomposites incorporating TiO_2, Sens. Actuators B 135 (2008) 7–12.
[3] K.V. Gurav, P.R. Deshmukh, C.D. Lokhande, LPG sensing properties of Pd-sensitized vertically aligned ZnO nanorods, Sens. Actuators B 151 (2011) 365–369.
[4] J.C. Kim, H.K. Jun, J. Huh, D.D. Lee, Tin oxide-based methane gas sensor promoted by alumina-supported Pd catalyst, Sens. Actuators B 45 (1997) 271–277.
[5] L. de Angelis, R. Riva, Selectivity and stability of tin dioxide sensor for methane, Sens. Actuators B 28 (1995) 25–29.
[6] G. Tournier, C. Pijolat, R. Lalauze, B. Patissier, Selective detection of CO and CH_4 with gas sensors using SnO_2 doped with palladium, Sens. Actuators B 26 (1995) 24–28.
[7] J. Wang, B. Hokkanen, U. Burghaus, Adsorption of iso-butane on ZnO(0 0 0 1)–Zn, Surf. Sci. 600 (2006) 4855–4859.
[8] T. Mazingue, L. Escoubas, L. Spalluto, F. Flory, P. Jacquouton, A. Perrone, E. Kaminska, A. Piotrowska, I. Mihailescu, P. Atanasov, Optical characterizations of ZnO, SnO_2, and TiO_2 thin films for butane detection, Appl. Opt. 45 (2006) 1425.
[9] T. Mazingue, L. Escoubas, L. Spalluto, F. Flory, G. Socol, C. Ristoscu, E. Axente, S. Grigorescu, I.N. Mihailescu, N.A. Vainos, Nanostructured ZnO coatings grown by pulsed laser deposition for optical gas sensing of butane, J. Appl. Phys. 98 (2005) 074312.
[10] O. Lupan, G. Chai, L. Chow, A single ZnO tetrapod-based sensor, Sens. Actuators B 141 (2009) 511–517.
[11] J. Joo, D. Lee, M. Yoo, S. Jeon, ZnO nanorod-coated quartz crystals as self-cleaning thiol sensors for natural gas fuel cells, Sens. Actuators B 138 (2009) 485–490.
[12] J.H. Kim, J.S. Sung, Y.M. Son, A.A. Vasiliev, V.V. Malyshev, E.A. Koltypin, A.V. Eryshkin, D.Yu. Godovski, A.V. Pisyakov, S.S. Yakimov, Propane:butane semiconductor gas sensor with low power consumption, Sens. Actuators B 44 (1997) 452–457.
[13] E. Flitsiyan, C. Swartz, R.E. Peale, O. Lupan, L. Chernyak, L. Chow, W.G. Vernetson, Z. Dashevsky, Neutron transmutation doping and radiation hardness for solution-grown bulk and nano-structured ZnO, Mater. Res. Soc. Symp. Proc. 1108 (2009) 55–60.
[14] V.V. Ursaki, E.V. Rusu, A. Sarua, M. Kuball, G.I. Stratan, A. Burlacu, I.M. Tiginyanu, Optical characterization of hierarchical ZnO structures grown with a simplified vapour transport method, Nanotechnology 18 (2007) 215705.
[15] H. Kind, H. Yan, B. Messer, M. Law, P. Yang, Nanowire ultraviolet photodetectors and optical switches, Adv. Mater. 14 (2002) 158.
[16] O. Lupan, L. Chow, G. Chai, B. Roldan, A. Naitabdi, A. Schulte, H. Heinrich, Nanofabrication and characterization of ZnO nanorod arrays and branched microrods by aqueous solution route and rapid thermal processing, Mater. Sci. Eng. B 145 (2007) 57–66.
[17] D. Polsongkram, P. Chamninok, S. Pukird, et al., Effect of synthesis conditions on the growth of ZnO nanorods via hydrothermal method, Physica B: Condens. Mater. 403 (2008) 3713–3717.
[18] V.M. Markushev, V.V. Ursaki, M.V. Ryzhkov, C.M. Briskina, I.M. Tiginyanu, E.V. Rusu, A.A. Zakhidov, ZnO lasing in complex systems with tetrapods, Appl. Phys. B 93 (2008) 231–238.
[19] O. Lupan, L. Chow, G. Chai, L. Chernyak, O. Lopatiuk-Tirpak, H. Heinrich, Focused-ion-beam fabrication of ZnO nanorod-based UV photodetector using the in situ lift-out technique, Phys. Stat. Sol. A 205 (2008) 2673–2678.
[20] O. Lupan, G. Chai, L. Chow, G. Emelchenko, H. Heinrich, V.V. Ursaki, A. Gruzintsev, I.M. Tiginyanu, A.N. Redkin, Ultraviolet photoconductive sensor based on single ZnO nanowire, Phys. Stat. Sol. A: Appl. Mater. 207 (2010) 1735–1740.
[21] G. Chai, O. Lupan, L. Chow, H. Heinrich, Crossed zinc oxide nanorods for ultraviolet radiation detection, Sens. Actuators A 150 (2009) 184–187.
[22] L. Chow, FIB fabrication of ZnO nanotetrapod and cross-sensor, Phys. Stat. Sol. B 247 (2010) 1628–1632.
[23] B.K. Meyer, H. Alves, D.M. Hofmann, W. Kriegseis, D. Forster, F. Bertram, J. Christen, A. Hoffmann, M. Strassburg, M. Dworzak, U. Haboeck, A.V. Rodina, Bound exciton and donor-acceptor pair recombinations in ZnO, Phys. Stat. Sol. B 241 (2004) 231–260.
[24] V.V. Ursaki, I.M. Tiginyanu, V.V. Zalamai, E.V. Rusu, G.A. Emelchenko, V.M. Masalov, E.N. Samarov, Multiphonon resonant Raman scattering in ZnO crystals and nanostructured layers, Phys. Rev. B 70 (2004) 155204.
[25] A. Kaschner, U. Haboeck, M. Strassburg, M. Strassburg, G. Kaczmarczyk, A. Hoffmann, C. Thomsen, A. Zeuner, H.R. Alves, D.M. Hofmann, B.K. Meyer, Nitrogen-related local vibrational modes in ZnO:N, Appl. Phys. Lett. 80 (2002) 1909–1911.
[26] Th. Pauporté, V.V. Ursaki, I.M. Tiginyanu, Highly luminescent columnar ZnO films grown directly on n- Si and p-Si substrates by low-temperature electrochemical deposition, Opt. Mater. 33 (6) (2011) 914–919.
[27] M. Rajalakshmi, A.K. Arora, B.S. Bendre, S. Mahamuni, Optical phonon confinement in zinc oxide nanoparticles, J. Appl. Phys. 87 (2000) 2445–2448.
[28] J. Serrano, F.G. Manjon, A.H. Romero, F. Widulle, R. Lauck, M. Cardona, Dispersive phonon linewidths: the E-2 phonons of ZnO, Phys. Rev. Lett. 90 (2003) 055510.
[29] O. Lupan, G. Chai, L. Chow, Fabrication of ZnO nanorod-based hydrogen gas nanosensor, Microelectron. J. 38 (2007) 1211–1216.
[30] O. Lupan, V.V. Ursaki, G. Chai, L. Chow, G.A. Emelchenko, I.M. Tiginyanu, A.N. Gruzintsev, A.N. Redkin, Selective hydrogen gas nanosensor using individual ZnO nanowire with fast response at room temperature, Sens. Actuators B 144 (2010) 56–66.
[31] T. Koerts, R.A. van Santen, The reaction path for recombination of surface CH_x species, J. Mol. Catal. 70 (1991) 119–127.
[32] T. Koerts, R.A. van Santen, A low temperature reaction sequence for methane conversion, J. Chem. Soc. Chem. Commun. 18 (1991) 1281.
[33] O. Lupan, G. Chai, L. Chow, Novel hydrogen gas sensor based on single ZnO nanorod, Microelectron. Eng. 85 (2008) 2220–2225.
[34] S. Saito, M. Miyayama, K. Kuomoto, H. Yanagida, Gas sensing characteristic of porous ZnO and Pt/ZnO ceramics, J. Am. Ceram. Soc. 68 (1985) 40–43.
[35] M.S. Arnold, P. Avouris, Z.W. Pan, Z.L. Wang, Field-effect transistors based on single semiconducting oxide nanobelts, J. Phys. Chem. B 107 (2003) 659–663.
[36] A. Kolmakov, M. Moskovits, Chemical sensing and catalysis by one-dimensional metal–oxide nanostructures, Annu. Rev. Mater. Res. 34 (2004) 151–180.
[37] L. Sun, F. Qiu, B. Quan, Investigation of a new catalytic combustion-type CH_4 gas sensor with low power consumption, Sens. Actuators B 66 (2000) 289–292.
[38] O. Lupan, B. Roldan Cuenya, H. Heinrich, E.E. Yakimov, G.A. Emelchenko, V.V. Ursaki, G. Chai, L.K. Ono, Synthesis and characterization of ZnO nanowires for nanosensor applications, Mater. Res. Bull. 45 (8) (2010) 1026–1032.

Biographies

Guangyu Chai is the Research Director at Apollo Technologies, Inc., Orlando, FL, USA. He received his B.S. in physics in 1999 from the Peking University, Beijing, China. He received Ph.D. in Condensed Matter Physics from University of Central Florida, Orlando, FL, USA in 2004. Research interests: ZnO nanorod sensors; individual carbon nanotube devices, focused ion beam fabrication of nanodevices.

Oleg Lupan received his M.S. in microelectronics and semiconductor devices from the Technical University of Moldova (TUM) in 1993. He received his Ph.D. in solid state electronics, microelectronics and nanoelectronics from the Institute of Applied Physics, Academy of Sciences of Republic of Moldova in 2005. His post-doctorate research activities were carried out at the French CNRS, Paris, France and University of Central Florida, USA. He was an invited scientist at the French CNRS, Paris, France. He received his Doctor habilitate degree in 2011 from the Institute of Electronic Engineering and Nanotechnologies of Academy of Sciences of Moldova. He is an Associate Professor and researcher scientist in solid state electronics, microelectronics and nanoelectronics at the Department of Microelectronics and Semiconductor Devices of the TUM. He is a visiting research professor during Spring semesters at the Department of Physics University of Central Florida, USA. His current research interests range over semiconducting oxides micro-nano-architectures and thin films for chemical sensors, optoelectronic devices and solar cells; nanotechnologies with self-assembly, chemical and electrochemical depositions; development and investigation of novel micro-nano-devices.

Emil V. Rusu received his M.S. degree from the Moldavian State University in 1965. He received his Ph.D. degree in semiconductor Physics from Institute of Applied Physics, Academy of Sciences of Moldova in 1974, and his Doctor habilitate degree in 1993 also from this institute. From 1992 to 2009, he worked the Institute of Applied Physics. Since 2009 he works at the Institute of Electronic Engineering and Nanotechnology of the Academy of Sciences of Moldova. His research interests are in the field of the elaboration of technological processes for the growth of bulk

oxide and nanostructured materials, conducting transparent films, nanostructures and their application in electrical and photonic devices.

Gheorghe I. Stratan received his M.S. degree from the Moldavian State University in 1965, and received his Ph.D. degree in semiconductor Physics from the Moldavian State University in 1992. From 1999 to 2009, he worked at the Institute of Applied Physics. Since 2009 he works at the Institute of Electronic Engineering and Nanotechnology of the Academy of Sciences of Moldova. His research interests are in the field of semiconductor materials, nanostructures and their application in optoelelectronic and photonic devices.

Veaceslav V. Ursaki received his M.S. degree from the Moscow Institute of Physics and Engineering in 1979. He received his Ph.D. degree in Semiconductor Physics from Lebedev Institute of Physics, Academy of Sciences of U.S.S.R., in 1986, and his Doctor habilitate degree in 1998 from the Institute of Applied Physics of the Academy of Sciences of Moldova. From 1986 he works at the Institute of Applied Physics of the Academy of Sciences of Moldova. His research interests are in the field of optical properties of semiconductor materials, lasing effects in solid state nanostructures, optoelectronic and photonic properties of nanostructures and nanocomposite materials.

Victor Şontea received his M.S. degree in microelectronics and semiconductor devices from the Polytechnic Institute of Chişinău, Moldova in 1973. He received his Ph.D. degree in Semiconductor Physics from the Institute of Applied Physics of the Academy of Sciences of Moldova of U.S.S.R., in 1982. He was promoted to professor in 1996. Since 1973 he works at the Technical University of Moldova (TUM). His research interests are in the Microelectronics, physics and technology of materials, semiconductor devices and micro-nano-electronics, engineering of micro-nano-electronics and biomedical devices.

Hani M.M. Khallaf is a lecturer at College of Sciences, El-Minia University. He received his B.S. in physics in 1998 from the Department of Physics, El-Minia University, Egypt. He received M.Sc. in 2005 and Ph.D. in 2009 in Condensed Matter Physics from University of Central Florida, Orlando, FL, USA. In 2010 he joined the Nanophotonic Device Research Group at CREOL; The College of Optics & Photonics, University of Central Florida as a post-doctoral research associate. Research interests: liquid phase deposition/chemical bath deposition of group II–VI semiconductor thin film materials for solar cells applications, organic photovoltaics.

Lee Chow is a Professor at the Department of Physics University of Central Florida Orlando. He received his B.S. in physics in 1972 from the National Central University, Taiwan. He received Ph.D. in Physics from Clark University, Worcester, MA, USA in 1981. In 1981–1982 he was a postdoc in physics at the University of North Carolina, Chapel Hill, NC. He joined University of Central Florida in 1983 as an assistant Professor, and was promoted to associate professor in 1988 and to professor in 1998. Areas of expertise: Chemical bath deposition, nanofabrications of carbon nanotubes and metal oxides, diffusion in semiconductors, high T_c thin film, hyperfine interactions, high pressure physics, and thin films.